

Assessing the structure of membrane proteins: combining different methods gives the full picture

Henning Stahlberg, Andreas Engel, and Ansgar Philippsen

Abstract: The rotor stoichiometry of F-ATPases has been revealed by the combined approaches of X-ray diffraction (XRD), electron crystallography, and atomic force microscopy (AFM). XRD showed the rotor from the yeast mitochondrial F-ATPase to contain 10 subunits. AFM was used to visualize the tetradecameric chloroplast rotors, and electron crystallography and AFM together revealed the rotors from *Ilyobacter tartaricus* to be composed of 11 subunits. While biochemical methods had determined an approximate stoichiometric value, precise measurements and new insights into a species-dependent rotor stoichiometry became available by applying the three structural tools together. The structures of AQP1, a water channel, and GlpF, a glycerol channel, were determined by electron crystallography and XRD. The combination of both of these structural tools with molecular dynamics simulations gave a differentiated description of the mechanisms determining the selectivity of water and glycerol channels. This illustrates that the combination of different methods in structural biology reveals more than each method alone.

Key words: AQP1, GlpF, F-ATPase, XRD, electron crystallography, AFM.

Résumé : La stoechiométrie des F-ATPases a été déterminée par des approches combinées de cristallographie par diffraction de rayons X (DRX), cristallographie électronique et microscopie des forces atomiques (MFA). La DRX a montré que le rotor de l'ATPase F mitochondriale de la levure est constitué de 10 sous-unités. La MFA a été utilisée pour visualiser les rotors tétradécamériques des chloroplastes et l'association de la cristallographie électronique et de la MFA a permis de montrer que les rotors de *Ilyobacter tartaricus* sont constitués de 11 sous-unités. Alors qu'une valeur stoechiométrique approximative avait été déterminée par des méthodes biochimiques, des mesures précises et de nouvelles données concernant la stoechiométrie des rotors selon les espèces ont été obtenues en utilisant ces trois outils ensemble. Les structures de AQP1, un canal de l'eau, et de GlpF, un canal du glycérol, ont été déterminées par cristallographie électronique et DRX. La combinaison de ces deux outils d'études structurales avec des simulations de dynamique moléculaire a permis d'obtenir une description des différences qui distinguent les mécanismes déterminant la sélectivité du canal de l'eau et la sélectivité du canal du glycérol. Cela démontre que la combinaison de différentes méthodes de biologie structurale révèle plus de choses que chacune de ces méthodes seule.

Mots clés : AQP1, GlpF, F-ATPase, diffraction de rayons X, DRX, cristallographie électronique, microscopie des forces atomiques, MFA.

[Traduit par la Rédaction]

Introduction

Structural biology is a multidisciplinary science whose goal is to assess the structure and function of biomolecules and their supermolecular assemblies by different techniques. These include X-ray diffraction (XRD), nuclear magnetic resonance (NMR), transmission electron microscopy, atomic force microscopy (AFM), and molecular dynamics simulations. Each technique can provide information on special as-

pects of a biological question. However, the full picture emerges only when results from different methods are combined.

Although XRD and NMR can determine the atomic structures of biomolecules at high speed, progress in membrane protein structure determination is slow, mainly due to the fact that membrane proteins are often unstable when extracted from the native lipidic environment. Electron crystallography and AFM, however, allow the structure of a

Received 18 June 2002. Revised 12 August 2002. Accepted 20 August 2002. Published on the NRC Research Press Web site at <http://bcf.nrc.ca> on 27 September 2002.

H. Stahlberg, A. Engel,¹ and A. Philippsen. M.E. Müller Institute, Biozentrum, University of Basel, Klingelbergstrasse 70, CH-4056 Basel, Switzerland.

¹Corresponding author (e-mail: Andreas.Engel@unibas.ch).

Fig. 1. Stoichiometries of the F_0 rotors of F-ATPases from bacteria, mitochondria, and chloroplasts determined by electron crystallography (bacteria, top half of panel), XRD (mitochondria), and AFM (bacteria (bottom half of panel) and chloroplasts (the lines indicate the subunits)). Surprisingly, a different aggregation number was found for each studied system. The mitochondrial ATPase representation was prepared with DINO (www.dino3d.org).

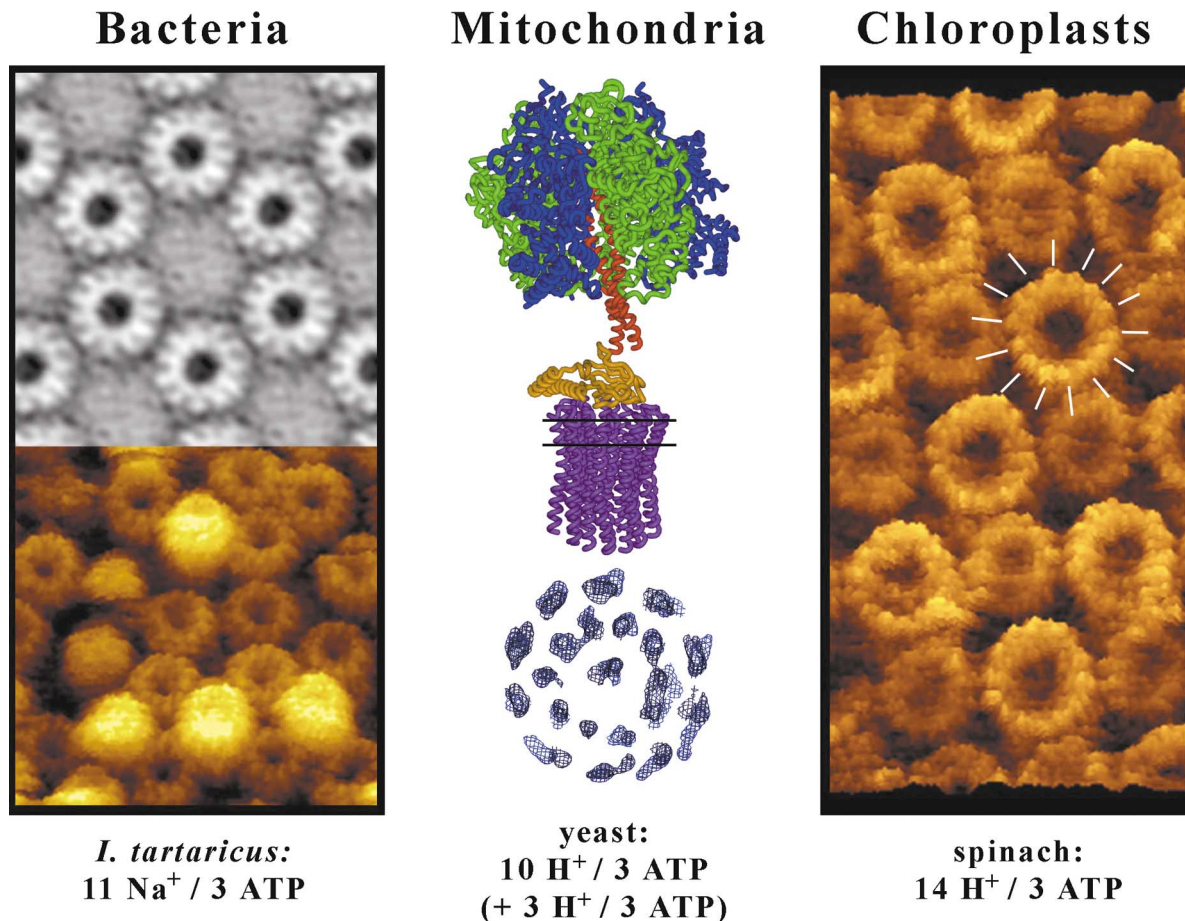


Table 1. Timeline for structure determination of water and glycerol channels.

Protein	PDB code	Resolution, method	Publication	Date of PDB deposition	PDB release
AQP1 (human rbc)	1FQY	3.8 Å, cryoEM	Murata et al. 2000 (Oct. 5)	Sept. 7, 2000	Oct. 18, 2000
GlpF (<i>E. coli</i>)	1FX8	2.2 Å, XRD	Fu et al. 2000 (Oct. 20)	Sept. 25, 2000	Nov. 1, 2000
AQP1 (human rbc)	1IH5	3.7 Å, cryoEM	Ren et al. 2001 (Feb. 13)	Apr. 18, 2001	Apr. 25, 2001
AQP1 (human rbc)	1H6I	3.5 Å, cryoEM + MD	de Groot et al. 2001 (Aug. 31)	June 15, 2001	Dec. 13, 2001
AQP1 (bovine rbc)	1J4N	2.2 Å, XRD	Sui et al. 2001 (Dec. 20)	Oct. 19, 2001	Mar. 27, 2002

Note: PDB, protein data bank (Berman et al. 2000); rbc, red blood cells; cryoEM, electron crystallography; MD, molecular dynamics simulations.

membrane protein to be studied, when it is embedded in a lipid bilayer.

Two examples are presented here that demonstrate the power of integrating the information acquired by different techniques.

First case: stoichiometric ratio of F-ATPases

F-ATP synthases are nanomachines that produce ATP while consuming the energy of a proton or sodium gradient across a biological membrane or hydrolyze ATP to restore

the gradient (Junge et al. 2001). The flow of these ions across the membrane propels the smallest existing rotors, which are composed of n subunits and are integrated in the membrane-resident part F_0 of the F-ATPase. The rotation of these 5- to 7-nm large cylindrical protein complexes is transmitted to a long rod, which drives the synthesis of ATP from ADP and P_i in the extramembranous part F_1 of the same enzyme. The latter exhibits a highly conserved structure comprising three catalytic sites arranged around a threefold axis (Abrahams et al. 1994), which strongly suggests that three ATPs are synthesized for each full rotation of the long rod.

Therefore, the proton to ATP ratio appears to be directly linked to the stoichiometry of the rotor, which is thought to rotate by $2\pi/n$ per translocated cation.

Biochemical determination of the proton to ATP ratio proved to be difficult. Four protons per ATP is the currently accepted overall value for mitochondria (Ferguson and Sorgato 1982; Ferguson 2000) as well as chloroplasts (Pänke and Rumberg 1997; van Walraven et al. 1996). The prediction of 12 *c*-subunits in the F_0 ring in *Escherichia coli*, based on genetic fusion of *c*-subunits and cross-linking experiments (Jones and Fillingame 1998), is in perfect agreement with this proton to ATP ratio of four (12 protons would cause a 360° rotation of the *c*-ring and release three ATP molecules from F_1). However, this simplistic view does not account for transport systems for ADP, P_i , and ATP in mitochondria or the chemical potential of the ATP gradient in chloroplasts. Nevertheless, several models of the rotor have been built based on the NMR structure of the *c*-subunit (Dmitriev et al. 1999; Rastogi and Girvin 1999). Therefore, other stoichiometries for the rotary motor from different sources appeared to be counterintuitive.

F-ATPase from yeast mitochondria

The first solid evidence, contradicting the dodecameric *c*-ring model, was the structure of the nearly complete yeast F-ATPase (Stock et al. 1999), determined at 4.0 Å (1 Å = 0.1 nm) resolution by XRD from three-dimensional crystals. This work revealed the existence of only 10 *c*-subunits in the F_0 rotor part.

As subsequently discussed (Ferguson 2000), this number of 10 *c*-subunits is not in strong contradiction to the predicted ratio of four protons per synthesized ATP because one proton is needed for the transport of ATP out into the cytosol and ADP, as well as P_i , back into the mitochondrial matrix. The synthesis of three ATP would therefore consume 10 protons at the F-ATPase plus three protons for the delivery. This corresponds to a proton to ATP ratio of 4.33.

F-ATPase from chloroplasts

The rotors of F_0 -ATPases from chloroplasts have an unusually high stability. This allowed their purification and reconstitution into regularly packed membrane sheets. Since the crystal order was poor, AFM was employed to visualize the rotors embedded in the lipid bilayer (Seelert et al. 2000). Unexpectedly, the images clearly showed rings with 14 subunits *III* (corresponding to the *c*-subunits in other F-ATPases). A consumption of 14 protons for three synthesized ATP corresponds to a proton to ATP ratio of 4.67.

F-ATPase from *Ilyobacter tartaricus*

The sodium-driven F-ATPase from *Ilyobacter tartaricus* also exhibits a stable rotor, which could be purified and reconstituted into lipid membranes without interruption of the rings. In this case, well-ordered two-dimensional crystals of *c*-rings could be grown. This allowed crystallographic analysis by electron microscopy, yielding a projection map at 6.9 Å resolution of these rotors (Stahlberg et al. 2001). This time, the rotors revealed 11 subunits, which was also shown by AFM of the same two-dimensional crystals. A consump-

tion of 11 Na^+ for three generated ATP corresponds to a proton to ATP ratio of 3.67.

Discussion

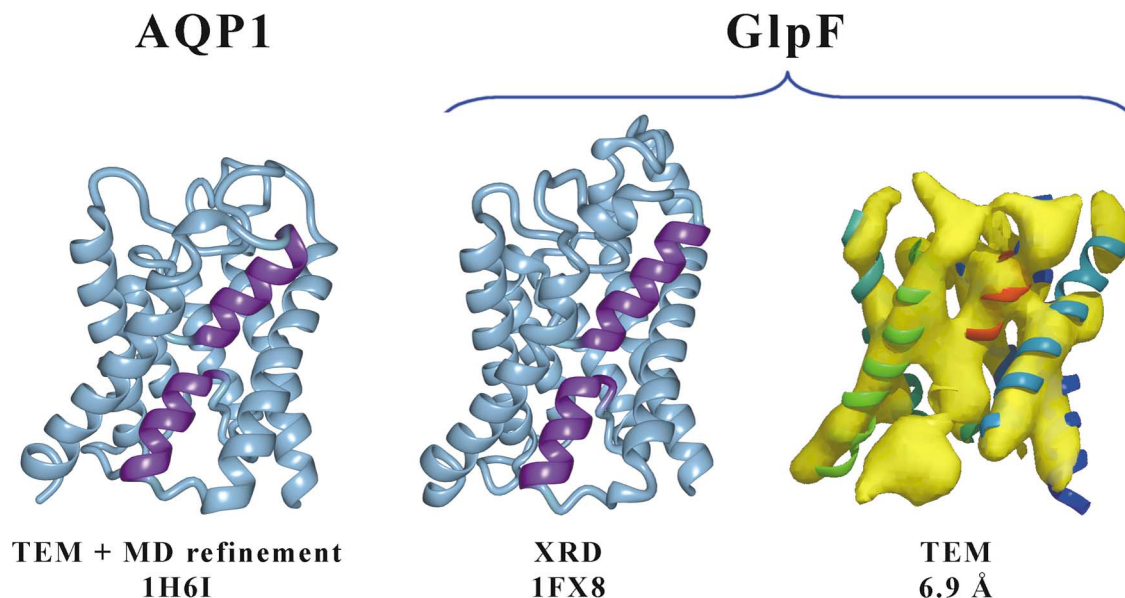
The stoichiometry of F-ATPases had been a matter of intensive discussion for decades. Instead of giving a single number as the answer to this discussion, the results from XRD, AFM, and electron crystallography revealed three different proton to ATP ratios for three different organisms (Fig. 1). The ratios of 3.33, 4.67, and 3.67 for the mitochondrial, chloroplast, and bacterial enzymes have in common that they are nonintegral. As proposed earlier, this symmetry mismatch facilitates rotation (Stock et al. 2000; also see Simpson et al. 2000). The model of a dynamically adapting enzyme that adjusts the stoichiometry of the *c*-ring to establish a required gear ratio (Schemidt et al. 1998) is not supported by the high quality of the crystals that could be grown from the mitochondrial and bacterial enzymes. These results rather indicate a unique, species-specific design of the rotor with a constant *c*-subunit stoichiometry. In all intact rings of the chloroplast as well as the bacterial enzyme visualized by AFM, no variation of the stoichiometry has been found. In addition, the analysis of broken rings revealed a constant curvature, suggesting the ring stoichiometry to be subunit dependent (Müller et al. 2001).

Second case: aquaporins

Aquaporins are ubiquitous membrane channels found in bacteria, plants, and animals. A decade ago, Peter Agre and co-workers demonstrated aquaporin-1 (AQP1) to mediate the passage of water across biological membranes (Preston et al. 1992). Since then, more than 300 different members of the family of water channel proteins have been identified (Engel and Stahlberg 2002). Phylogenetic analyses reveal the existence of two subfamilies within the water channel superfamily: the AQP cluster, which is composed of channels permeable to water, and the GLP cluster, combining channels that facilitate the permeation of glycerol and other small, nonionic solutes.

The structure of AQP1 was first analyzed by electron crystallography, revealing three-dimensional density maps at a resolution of 6–7 Å (Cheng et al. 1997; Li et al. 1997; Walz et al. 1997). Three years later, electron crystallography provided the first atomic structure of this channel at a resolution of 3.8 Å (Murata et al. 2000; Table 1, PDB entry 1FQY; Fig. 2). This structure allowed the water channel pathway and the channel lining residues to be described and provided an explanation for the high permeation rate of water with simultaneous blockage of protons. This property is remarkable, since a one-dimensional hydrogen-bonded file of water molecules does conduct protons by the Grotthuss effect (Grotthuss 1806; Agmon 1995; also see Marx et al. 1999; Pomes and Roux 1996, 2002). The atomic structure suggested the two asparagines Asn76 and Asn192 at the central narrowing of the channel to interrupt the proton wire by acting as strong hydrogen bond donors. Favorable orientation of passing water molecules is ensured by the field resulting from the two highly conserved short helices that form the channel. Another atomic structure of AQP1 deter-

Fig. 2. Atomic models of AQP1 and GlpF determined by electron crystallography with homology modeling refinement (1H6I) and by XRD (1FX8). The 6.9-Å density of GlpF was determined by electron crystallography from data collected within 10 days.



mined by electron crystallography at 3.7 Å has been published more recently (Ren et al. 2001; Table 1, PDB entry 1IH5).

The glycerol channel GlpF from *E. coli* was the second available atomic structure of a water channel superfamily member. GlpF was solved in the presence of glycerol by XRD at a resolution of 2.2 Å, giving a detailed insight into the nature of the selective permeability for linear carbohydrates (Fu et al. 2000; Table 1, PDB entry 1FX8; Fig. 2). The GlpF structure reveals an amazing homology to the AQP1 structure. The root mean square deviation between 1FX8 and 1FYQ of the backbone atoms in the helical regions amounts to 1.75 Å only. In spite of this similarity, the pore has a significantly larger diameter than that of AQP1, accommodating three glycerol molecules associated with water in the crystals grown in 2 M glycerol. The hydroxyl groups of these glycerols are both hydrogen bond acceptors from successive NHs facing the channel and hydrogen bond donors to carbonyls. The glycerol's alkyl backbone, however, is wedged against the hydrophobic residues lining the pore. Amphiphilicity, size, and a highly specific network of hydrogen bond donors and acceptors define the pore specificity. As demonstrated by permeation experiments with alditols, this pore exhibits a stereoselective preference for glycerol and linear carbohydrates, as expected from the disposition of hydrogen-bonding sites in the pore.

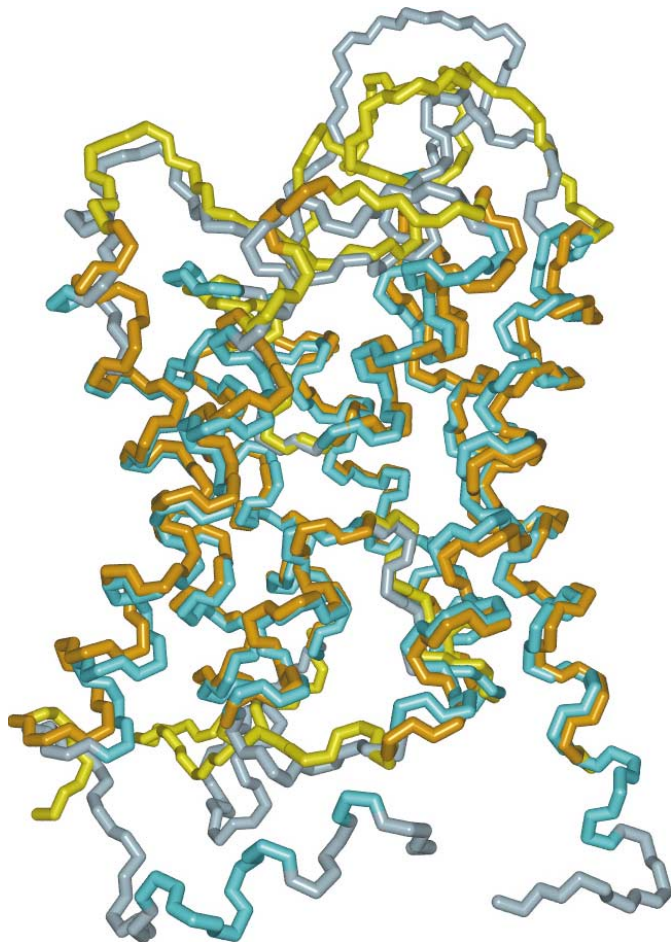
A 6.9-Å structure of the glycerol channel GlpF was obtained by electron crystallography from images recorded within 10 days and evaluated within 2 months. This map promoted the prediction of the channel amphipathicity and dimensions by homology modeling based on the AQP1 atomic model (Stahlberg et al. 2000) (Fig. 2). Although the results obtained by XRD are much more detailed, the latter work demonstrates the feasibility of fast structure determination by electron crystallography.

The structural homology of GlpF and AQP1 provided a solid basis to build an independent atomic structure of AQP1

by homology modeling, starting from the 2.2-Å GlpF structure. This model was subsequently refined against the 3.8-Å density map of AQP1 obtained by electron crystallography. This approach resulted in a significant improvement of the *R* factor from 39.9 to 36.7% and free *R* factor from 41.7 to 37.8% (de Groot et al. 2001; Table 1, PDB entry 1H6I). More importantly, however, the stability of this refined AQP1 structure during molecular dynamics simulations improved significantly (de Groot et al. 2001), making extensive numerical simulations possible to gain insight into the permeation of water. Such simulations were also achieved starting from the 2.2-Å GlpF structure after computational elimination of the three glycerols (de Groot and Grubmüller 2001). A wealth of information emerged from these numerical experiments on AQP1. First, water molecules were found to permeate the pore in an oriented manner, with their dipole pointing to the closer membrane surface and undergoing a 180° rotation upon passage of the highly conserved Asp-Pro-Ala (NPA) motifs in the center of the channel, promoting disruption of water–water hydrogen bonding. Second, a detailed characterization of the hydrogen bonding network identified a further site, where water–water hydrogen bonds are inhibited. It coincides with the smallest constriction of the pore at the highly conserved Arg195. Third, permeation rates measured in the numerical simulation turned out to be close to those determined by measuring swelling or shrinkage of proteoliposomes (Borgnia and Agre 2001). The numerical simulation of the GlpF deprived from the glycerols that were present in the initial structure also revealed orientation of water, but to a lesser extent. But these simulations showed minor conformational changes that reduced the channel diameter (de Groot and Grubmüller 2001), suggesting a possible explanation for the lower water permeability measured for GlpF as compared with AQP1 (Borgnia and Agre 2001).

Most recently, three new structures of GlpF, solved by XRD, were submitted to extensive molecular dynamics anal-

Fig. 3. Comparison of the atomic models of AQP1 determined by electron crystallography with homology-based refinement (1H6I, orange–yellow) and GlpF determined by XRD (1J4N, cyan – light blue). The alignment was done with SPDBV (www.expasy.ch/spdbv/) and has a root mean square deviation of 0.9 Å (transmembrane parts only).



yses (PDB entries 1LDI, 1LDA, and 1LDF; Tajkhorshid et al. 2002). These experiments revealed the orientation of the channel-traversing water molecules in GlpF as pronounced as in AQP1. Most importantly, the half-helix dipoles and the conserved Asn76 and Asn192 were found to have a strong effect, as predicted by Murata et al. (2000), because the water orientation became random when dipoles and the charges on the NH₂ groups of the NPA asparagines were turned off computationally. Several resident water molecules were revealed by the 2.7-Å map of water-bound GlpF and found in locations compatible with those predicted from numerical simulations. As expected, one water molecule is observed between Asn68 and Asn203, where hydrogen-bonding interaction between water and the pore is pronounced (de Groot and Grubmüller 2001; Tajkhorshid et al. 2002).

Finally, XRD analysis has provided the 2.2-Å structure of bovine AQP1 (Sui et al. 2001; Table 1, PDB entry 1J4N). The transmembrane regions of this structure confirm the refined structure (1H6I; de Groot et al. 2001) derived from electron crystallographic data (Murata et al. 2000) and X-ray data (Fu et al. 2000) and subsequently tested in molecular

dynamics simulations (root mean square deviation of 0.9 Å) (Fig. 3). However, the loop regions of the bovine AQP1 structure (1J4N) show significant differences from the human AQP1 structure (1H6I). These differences may partly be explained by the protein–protein contacts during the three-dimensional crystal growth (Fotiadis et al. 2002). Fortunately, the overall quality of electron crystallographic data can now be fully evaluated using the much higher resolution structure from X-ray analyses. This is reported elsewhere (Fujiyoshi et al. 2002).

Discussion

The structural analyses of two representatives for the AQP and GLP clusters within the water channel superfamily reviewed here show the efficiency of the combination of XRD, electron crystallography, and molecular dynamics simulations. They also demonstrate the validity of the approach to refine a 3.8-Å resolution data set from electron crystallography by homology modeling using data from XRD, applying molecular dynamics simulations, and incorporating all available information about the protein from multiple sequence alignments (Heymann and Engel 2000).

Conclusion

While the high resolution of XRD provides the static information for understanding the function of a biomolecule, it is the molecular dynamics simulation that now has reached maturity to deliver insight into the dynamics of biological processes. Electron crystallography is a valid approach for assessing the atomic structure of membrane proteins that have resisted three-dimensional crystallization experiments. The data now emerging from the work with AQP1 underline the quality of structural information acquired by electron crystallography. Finally, the atomic force microscope is hitherto the only instrument giving structural information at subnanometre resolution from a single biomolecule. While each method has its benefits, only the combination of these tools reveals the full picture.

Acknowledgements

We thank Daniela Stock for providing material for Fig. 2. This work was supported by the Swiss National Foundation, the M.E. Müller Foundation of Switzerland, the European Union Quality of Life and Management of Living Resources Project (grants QLRT-2000-00778 and QLRT-2000/00504 to A.E.), and the Human Frontier Science Program (grant RG0021/2000-M103 to A.E.).

References

- Abrahams, J.P., Leslie, A.G., Lutter, R., and Walker, J.E. 1994. Structure at 2.8 Å resolution of F₁-ATPase from bovine heart mitochondria. *Nature (London)*, **370**: 621–628.
- Agmon, N. 1995. The Grotthuss mechanism. *Chem. Phys. Lett.* **244**: 456–462.
- Berman, H.M., Westbrook, J., Feng, Z., Gilliland, G., Bhat, T.N., Weissig, H., Shindyalov, I.N., and Bourne, P.E. 2000. The protein data bank. *Nucleic Acids Res.* **28**: 235–242.

- Borgnia, M.J., and Agre, P. 2001. Reconstitution and functional comparison of purified GlpF and AqpZ, the glycerol and water channels from *Escherichia coli*. Proc. Natl. Acad. Sci. U.S.A. **98**: 2888–2893.
- Cheng, A., van Hoek, A.N., Yeager, M., Verkman, A.S., and Mitra, A.K. 1997. Three-dimensional organization of a human water channel. Nature (London), **387**: 627–630.
- de Groot, B.L., and Grubmüller, H. 2001. Water permeation across biological membranes: mechanism and dynamics of aquaporin-1 and GlpF. Science (Washington, D.C.), **294**: 2353–2357.
- de Groot, B.L., Engel, A., and Grubmüller, H. 2001. A refined structure of human aquaporin-1. FEBS Lett. **504**: 206–211.
- Dmitriev, O.Y., Jones, P.C., and Fillingame, R.H. 1999. Structure of the subunit *c* oligomer in the F₁F₀ ATP synthase: model derived from solution structure of the monomer and cross-linking in the native enzyme. Proc. Natl. Acad. Sci. U.S.A. **96**: 7785–7790.
- Engel, A., and Stahlberg, H. 2002. Aquaglyceroporins: channel proteins with a conserved core, multiple functions, and variable surfaces. Int. Rev. Cytol. **215**: 75–104.
- Ferguson, S.J. 2000. ATP synthase: what dictates the size of a ring? Curr. Biol. **10**: R804–R808.
- Ferguson, S.J., and Sorgato, M.C. 1982. Proton electrochemical gradients and energy-transduction processes. Annu. Rev. Biochem. **51**: 185–217.
- Fotiadis, D., Suda, K., Tittmann, P., Jenö, P., Philippsen, A., Müller, D.J., Gross, H., and Engel, A. 2002. Identification and structure of a putative Ca²⁺-binding domain at the C terminus of AQP1. J. Mol. Biol. **318**: 1381–1394.
- Fu, D., Libson, A., Miercke, L.J., Weitzman, C., Nollert, P., Krucinski, J., and Stroud, R.M. 2000. Structure of a glycerol-conducting channel and the basis for its selectivity. Science (Washington, D.C.), **290**: 481–486.
- Fujiyoshi, Y., Mitsuoka, K., de Groot, B., Philippsen, A., Grubmüller, H., Agre, P., and Engel, A. 2002. Structure and function of water channels. Curr. Opin. Struct. Biol. **12**: 509–515.
- Grotthuss, C.J.T.d. 1806. Sur la décomposition de l'eau et des corps qu'elle tient en dissolution à l'aide de l'électricité galvanique. Ann. Chim. **LVIII**: 54–74.
- Heymann, B., and Engel, A. 2000. Structural clues in the sequences of the aquaporins. J. Mol. Biol. **295**: 1039–1053.
- Jones, P.C., and Fillingame, R.H. 1998. Genetic fusions of subunit *c* in the F₀ sector of H⁺-transporting ATP synthase. J. Biol. Chem. **273**: 29 701 – 29 705.
- Junge, W., Panke, O., Cherepanov, D.A., Gumbiowski, K., Müller, M., and Engelbrecht, S. 2001. Inter-subunit rotation and elastic power transmission in F₀F₁-ATPase. FEBS Lett. **504**: 152–160.
- Li, H., Lee, S., and Jap, B.K. 1997. Molecular design of aquaporin-1 water channel as revealed by electron crystallography. Nat. Struct. Biol. **4**: 263–265.
- Marx, D., Tuckerman, M.E., Hutter, J., and Parrinello, M. 1999. The nature of the hydrated excess proton in water. Nature (London), **397**: 601–604.
- Müller, D.J., Dencher, N.A., Meier, T., Dimroth, P., Suda, K., Stahlberg, H., Engel, A., Seelert, H., and Matthey, U. 2001. ATP synthase: constrained stoichiometry of the transmembrane rotor. FEBS Lett. **504**: 219–222.
- Murata, K., Mitsuoka, K., Hirai, T., Walz, T., Agre, P., Heymann, J.B., Engel, A., and Fujiyoshi, Y. 2000. Structural determinants of water permeation through aquaporin-1. Nature (London), **407**: 599–605.
- Pänke, O., and Rumberg, B. 1997. Energy and entropy balance of ATP synthesis. Biochim. Biophys. Acta, **1322**: 183–194.
- Pomes, R., and Roux, B. 1996. Structure and dynamics of a proton wire: a theoretical study of H⁺ translocation along the single-file water chain in the gramicidin A channel. Biophys. J. **71**: 19–39.
- Pomes, R., and Roux, B. 2002. Molecular mechanism of H(+) conduction in the single-file water chain of the gramicidin channel. Biophys. J. **82**: 2304–2316.
- Preston, G.M., Carroll, T.P., Guggino, W.B., and Agre, P. 1992. Appearance of water channels in *Xenopus* oocytes expressing red cell CHIP28 protein. Science (Washington, D.C.), **256**: 385–387.
- Rastogi, V.K., and Girvin, M.E. 1999. Structural changes linked to proton translocation by subunit *c* of the ATP synthase. Nature (London), **402**: 263–268.
- Ren, G., Reddy, V.S., Cheng, A., Melnyk, P., and Mitra, A.K. 2001. Visualization of a water-selective pore by electron crystallography in vitreous ice. Proc. Natl. Acad. Sci. U.S.A. **98**: 1398–1403.
- Schmidt, R.A., Qu, J., Williams, J.R., and Brusilow, W.S. 1998. Effects of carbon source on expression of F₀ genes and on the stoichiometry of the *c* subunit in the F₁F₀ ATPase of *Escherichia coli*. J. Bacteriol. **180**: 3205–3208.
- Seelert, H., Poetsch, A., Dencher, N.A., Engel, A., Stahlberg, H., and Müller, D.J. 2000. Imaging the proton powered motor of chloroplast ATP synthase. Nature (London), **405**: 418–419.
- Simpson, A.A., Tao, Y., Leiman, P.G., Badasso, M.O., He, Y., Jardine, P.J., Olson, N.H., Morais, M.C., Grimes, S., Anderson, D.L., Baker, T.S., and Rossmann, M.G. 2000. Structure of the bacteriophage phi29 DNA packaging motor. Nature (London), **408**: 745–750.
- Stahlberg, H., Braun, T., de Groot, B., Philippsen, A., Borgnia, M.J., Agre, P., Kühlbrandt, W., and Engel, A. 2000. The 6.9 Å structure of GlpF: a basis for homology modeling of the glycerol channel from *Escherichia coli*. J. Struct. Biol. **132**: 133–141.
- Stahlberg, H., Müller, D.J., Suda, K., Fotiadis, D., Engel, A., Meier, T., Matthey, U., and Dimroth, P. 2001. Bacterial Na(+)-ATP synthase has an undecameric rotor. EMBO Rep. **2**: 229–233.
- Stock, D., Leslie, A.G., and Walker, J.E. 1999. Molecular architecture of the rotary motor in ATP synthase. Science (Washington, D.C.), **286**: 1700–1705.
- Stock, D., Gibbons, C., Arechaga, I., Leslie, A.G., and Walker, J.E. 2000. The rotary mechanism of ATP synthase. Curr. Opin. Struct. Biol. **10**: 672–679.
- Sui, H., Han, B.G., Lee, J.K., Walian, P., and Jap, B.K. 2001. Structural basis of water-specific transport through the AQP1 water channel. Nature (London), **414**: 872–878.
- Tajkhorshid, E., Nollert, P., Jensen, M.O., Miercke, L.J., O'Connell, J., Stroud, R.M., and Schulten, K. 2002. Control of the selectivity of the aquaporin water channel family by global orientational tuning. Science (Washington, D.C.), **296**: 525–530.
- van Walraven, H.S., Strotmann, H., Schwarz, O., and Rumberg, B. 1996. The H⁺/ATP coupling ratio of the ATP synthase from thiol-modulated chloroplasts and two cyanobacterial strains is four. FEBS Lett. **379**, 309–313.
- Walz, T., Hirai, T., Murata, K., Heymann, J.B., Mitsuoka, K., Fujiyoshi, Y., Smith, B.L., Agre, P., and Engel, A. 1997. The three-dimensional structure of aquaporin-1. Nature (London), **387**: 624–627.